

EVLA NOVA PROJECT OBSERVATIONS OF THE CLASSICAL NOVA V1723 AQUILAE

MIRIAM I. KRAUSS, LAURA CHOMIUK^{1, 2}, MICHAEL RUPEN, NIRUPAM ROY², AND AMY J. MIODUSZEWSKI
 National Radio Astronomy Observatory, Socorro, NM 87801
 mkrauss, lchomiuk, mrupen, amiodusz, and nroy@nrao.edu

J. L. SOKOŁOSKI
 Columbia Astrophysics Laboratory, Columbia University, New York, NY 10027
 jsokoloski@astro.columbia.edu

THOMAS NELSON³ AND KOJI MUKAI
 CRESST and X-ray Astrophysics Laboratory, NASA/GSFC, Greenbelt, MD 20771
 and Center for Space Science and Technology, University of Maryland Baltimore County, Baltimore, MD 21250
 thomas.nelson and koji.mukai-1@nasa.gov

M. F. BODE
 Astrophysics Research Institute, Liverpool John Moores University, Twelve Quays House, Egerton Wharf, Birkenhead CH41 1LD
 mfb@astro.livjm.ac.uk

S. P. S. EYRES
 Jeremiah Horrocks Institute, University of Central Lancashire, Preston, PR1 2HE, UK
 spseyres@uclan.ac.uk

T. J. OBRIEN
 Jodrell Bank Centre for Astrophysics, University of Manchester, Manchester, UK M13 9PL
 tim.obrien@manchester.ac.uk
Draft version February 17, 2022

ABSTRACT

We present radio light curves and spectra of the classical nova V1723 Aql obtained with the Expanded Very Large Array (EVLA). This is the first paper to showcase results from the EVLA Nova Project, which comprises a team of observers and theorists utilizing the greatly enhanced sensitivity and frequency coverage of EVLA radio observations, along with observations at other wavelengths, to reach a deeper understanding of the energetics, morphology, and temporal characteristics of nova explosions. Our observations of V1723 Aql span 1–37 GHz in frequency, and we report on data from 14–175 days following the time of the nova explosion. The broad frequency coverage and frequent monitoring show that the radio behavior of V1723 Aql does not follow the classic Hubble-flow model of homologous spherically expanding thermal ejecta. The spectra are always at least partially optically thin, and the flux rises on faster timescales than can be reproduced with linear expansion. Therefore, any description of the underlying physical processes must go beyond this simple picture. The unusual spectral properties and light curve evolution might be explained by multiple emitting regions or shocked material. Indeed, X-ray observations from *Swift* reveal that shocks are likely present.

Subject headings: binaries: general — white dwarfs — novae, cataclysmic variables — stars: individual (V1723 Aql)

1. INTRODUCTION

Novae are the most common major stellar explosions in the Universe, resulting when the accretion of hydrogen onto the surface of a white dwarf leads to a thermonuclear runaway. Galactic novae occur relatively nearby and evolve on short timescales (months to years), making them excellent laboratories for understanding the accretion and outflow processes that influence a wide

range of astrophysical phenomena, from planetary nebulae to supernovae and active galactic nuclei. Radio continuum emission from classical novae has been observed for more than three decades (Hjellming et al. 1979; Seaquist & Palimaka 1977; Seaquist et al. 1980), and is generally thought to result from thermal free-free processes. Most novae observed in the radio have been understood as expanding, thermally-emitting shells of ejecta, though some show evidence of non-thermal emission as well (see Seaquist & Bode 2008 for a review). Radio continuum emission provides unique insights into the properties of this ejecta, since it is optically thick at much lower densities than other wavelengths (e.g., opti-

¹ Also Harvard-Smithsonian Astrophysical Observatory, Cambridge, MA 02139

² National Radio Astronomy Observatory Jansky Fellow

³ Current address: School of Physics and Astronomy, University of Minnesota, Minneapolis, MN 55455

Table 1
Observed 1–8 GHz Radio Flux Densities (mJy)^a

Date	MJD	Day ^a	Epoch	Frequency (GHz)					
				1.38	1.88	4.74	5.25	6.49	7.00
25 Sep 2010	55464.1	13.6	1	< 0.042 ^c	...	< 0.033 ^c	...
6 Oct 2010	55475.1	24.6	3	0.096±0.025	0.122±0.025	0.155±0.020	0.161±0.021
15 Oct 2010	55484.1	33.6	4	0.536±0.029	0.606±0.028	0.778±0.023	0.857±0.023
18 Oct 2010	55487.1	36.6	5	< 0.38	< 0.32	0.964±0.045	1.030±0.039	1.279±0.036	1.393±0.039
24 Oct 2010	55493.1	42.6	6	< 0.65	1.26±0.11	2.194±0.042	2.390±0.041	2.892±0.040	3.044±0.041
29 Oct 2010	55498.0	47.5	7	< 0.81	1.39±0.18	3.193±0.050	3.490±0.051	4.072±0.051	4.285±0.050
7 Nov 2010	55507.8	57.3	8	< 1.61	1.30±0.20	3.910±0.052	4.079±0.051	4.572±0.054	4.791±0.054
2 Dec 2010	55532.9	82.4	9	< 0.84	0.78±0.18	1.368±0.030	1.393±0.028	1.922±0.034	2.048±0.028
18 Dec 2010	55548.9	98.4	10	< 0.81	< 0.57	1.124±0.038	1.256±0.034	1.559±0.032	1.677±0.036
14 Jan 2011	55575.8	125.3	11	0.996±0.038	1.133±0.037	1.389±0.034	1.497±0.032
30 Jan 2011	55591.8	141.3	12	< 0.75	< 0.43	0.885±0.055	0.967±0.052	1.225±0.051	1.351±0.046
5 Mar 2011	55625.5	175.0	13	0.669±0.021	0.787±0.019	1.159±0.023	1.201±0.020

^a Quoted upper limits are 3σ .

^b Days from 11 September 2010 (MJD 55450.5).

^c Insufficient source flux to perform self-calibration.

cal emission), is not subject to extinction, and can provide a measure of the total ejecta mass, temperature and density profiles, and kinetic energy (Hjellming 1996).

The EVLA Nova Project, undertaken by a team including observers and theorists of radio, optical, and X-ray emission from novae, is embarking on a new era of observations of Galactic novae. The cornerstone of the EVLA Nova Project is EVLA light curves and spectra of unprecedented time resolution, frequency coverage, and sensitivity. We endeavor to monitor every new nova in the Galaxy which is closer than 5 kpc, producing high-quality radio light curves and spectra which allow us to compare, in exquisite detail, the radio properties of novae with current theory, and will also provide the data needed to go beyond the simple, standard models of radio emission from novae. In addition, we are utilizing information from high-energy observations, as well as very-long-baseline radio interferometry, to help synthesize a complete, multifrequency understanding of nova explosions.

Here, we present observations of the classical nova V1723 Aql, which was discovered in outburst on 2010 September 11; we take the time of the start of the outburst to be MJD 55450.5 (Yamanaka et al. 2010; Balam et al. 2010). It is highly reddened, and on the first day of the outburst the H_α emission line had a full-width at zero intensity of 3000 km s^{-1} (Yamanaka et al. 2010), from which we infer an expansion velocity for the nova ejecta of 1500 km s^{-1} . From a peak R-band magnitude of 13.43 on 11.6 September 2010 (Yamanaka et al. 2010), it took 20 days for the R-band flux to decrease by two magnitudes (Henden 2010), implying that V1723 Aql is a member of the “fast” nova speed class (Payne-Gaposchkin 1957).

We describe our EVLA radio and *Swift* X-ray observations and data reduction procedures in §2 and data analysis in §3. We discuss possible physical interpretations of our observations in §4.

2. OBSERVATIONS

2.1. EVLA Observations

We monitored V1723 Aql with the EVLA beginning on 2010 September 25, approximately two weeks after its initial optical discovery. Here, we present data from

observations taken through 2011 March 5; further observations are planned and will be published separately. Each monitoring epoch covers a wide range of frequencies; most epochs include data spanning 1–37 GHz. During the course of our monitoring, which comprises a total of 27 hours and 840 GB of raw data, the EVLA progressed through the DnC, C, CnB, and B configurations. All data were acquired with the widest possible bandwidths using the WIDAR correlator and the current 8-bit samplers: 2 GHz at each band except L and X, where we used the available 1 and 0.8 GHz of bandwidth.

For each band, we observed a standard flux-reference calibration source, either 3C48 or 3C286, as well as a phase reference calibrator, either J1822-0938 (8.6° away; 1–9 GHz) or J1851+0035 (4.5° away; 19–37 GHz). Processing was done with NRAO’s Common Astronomy Software Applications (CASA) and Astronomical Image Processing System (AIPS). For each package, the analysis path was the same: first, we obtained a band-pass solution using a bright calibration source (usually the flux calibrator). With this solution, we solved for the gain amplitude and phase, and scaled the phase calibration source’s amplitude from the flux calibration source’s values, using the “Perley-Butler 2010” flux density standard. Finally, we applied these gain solutions to V1723 Aql. We performed one round of phase-only self-calibration using a point source model at 19–37 GHz; at lower frequencies (since other nearby sources are present) we used an image of the field for reference and two to three rounds as needed for convergence. Errors on the flux include errors from gaussian fitting, the image rms noise, and systematic errors of 1% at low frequencies (1–9 GHz) and 3% at high frequencies (19–37 GHz). Since these data were taken during the commissioning phase of the EVLA, our estimates of the systematics are based on the apparent scatter in the broad-band spectra. These errors are included in all tables and figures. For analysis, we grouped our data into “epochs”, with observations included in a given epoch separated by no more than three days. Tables 1 and 2 list the flux densities at each epoch.

2.2. Swift Observations

On days 40.6 and 61.4, we obtained observations of V1723 Aql with the *Swift* satellite (Gehrels et al. 2004)

Table 2
Observed 8–37 GHz Radio Flux Densities (mJy)^a

Date	MJD	Day ^a	Epoch	Frequency (GHz)					
				8.24	8.73	20.1	25.6	28.2	36.5
25 Sep 2010	55464.1	13.6	1	< 0.09 ^d	...
3 Oct 2010	55472.1	21.6	2	0.43± 0.07 ^{c,d}	...
6 Oct 2010	55475.1	24.6	3	0.90± 0.10 ^d	...
15 Oct 2010	55483.1	32.6	4	2.46± 0.11 ^d	...
18 Oct 2010	55487.1	36.6	5	1.604±0.042	1.741±0.055
19 Oct 2010	55488.1	37.6	5	2.84± 0.09	3.89± 0.12	4.22± 0.14	4.64± 0.15
24 Oct 2010	55493.1	42.6	6	3.492±0.052	3.648±0.055
29 Oct 2010	55497.0	46.5	7	4.817±0.060	4.891±0.063	7.02± 0.21	7.87± 0.24	7.63± 0.23	8.94± 0.28
7 Nov 2010	55507.8	57.3	8	5.299±0.064	5.393±0.067	7.20± 0.23	8.12± 0.25	8.72± 0.27	9.20± 0.28
3 Dec 2010	55533.9	83.4	9	2.490±0.039	2.554±0.045	5.83± 0.18	7.07± 0.22	8.00± 0.25	9.56± 0.31
18 Dec 2010	55548.9	98.4	10	1.938±0.038	2.010±0.045
21 Dec 2010	55551.7	101.2	10	5.45± 0.16	7.09± 0.21	8.34± 0.26	10.98± 0.34
14 Jan 2011	55575.8	125.3	11	1.676±0.037	1.780±0.044	4.99± 0.15	6.09± 0.19	6.53± 0.20	8.51± 0.27
30 Jan 2011	55591.8	141.3	12	1.620±0.035	1.703±0.040	4.53± 0.14	6.22± 0.19	6.95± 0.22	8.91± 0.28
5 Mar 2011	55625.5	175.0	13	1.436±0.023	1.510±0.023	5.01± 0.15	7.07± 0.21	7.95± 0.24	11.05± 0.34

^a Quoted upper limits are 3σ .

^b Days from 11 September 2010 (MJD 55450.5).

^c Insufficient source flux to perform self-calibration.

^d Values are reported for 32.1 GHz.

of duration 3.0 and 5.5 ks. Each observation resulted in an exposure with the X-ray telescope (XRT) and an image with the Ultraviolet Optical Telescope (UVOT). We used the *Swift* data analysis routines in HEASoft version 6.10 throughout our analysis. The UVOT images were both obtained with the UVW1 filter, which has a central wavelength of 2600 Å and a FWHM of 693 Å (Poole et al. 2008). V1723 Aql was not detected in either UVOT image with a limiting UVW1 magnitude of 20.36 (20.65) in the first (second) observation.

The XRT was operated in photon counting mode during both observations. We produced cleaned level 2 event files by running the XRT reduction pipeline on the level 1 event files, retaining events with grades 0–12. We then used XSelect v2.4 to create spectra for each dataset. Source counts were extracted from 30''-radius circular region centered on V1723 Aql; background counts were extracted from a 95''-radius source free region. The ancillary response files (ARF) were generated using the task *xrtmkarf*, and were corrected for hot pixels and dead columns using an exposure map of each observation. Finally, we used the most recent response matrix file (RMF) appropriate for PC mode and event grades 0–12 from the *Swift* calibration database.

3. DATA ANALYSIS AND RESULTS

3.1. Radio Light Curves and Spectra

V1723 Aql's light curves are characterized by an initial steep rise until around day 50 ($S_\nu \propto t^{3.3}$ at 32.1 GHz), at which point there is a turnover and rapid decay at the lower frequencies (1–9 GHz) and flattening at 19 GHz and higher (Figure 1). In order to characterize the radio spectra, we fit simple power-law models to each epoch's 4–37 GHz spectrum; the spectra, along with fits and residuals, are shown in Figure 2. The fit residuals in some epochs suggest the presence of a spectral break, so we performed separate power-law fits to the lower (1–9 GHz) and higher (19–37 GHz) frequencies as well. In order to determine whether any improvement in fit was statistically significant, we performed F-tests for each

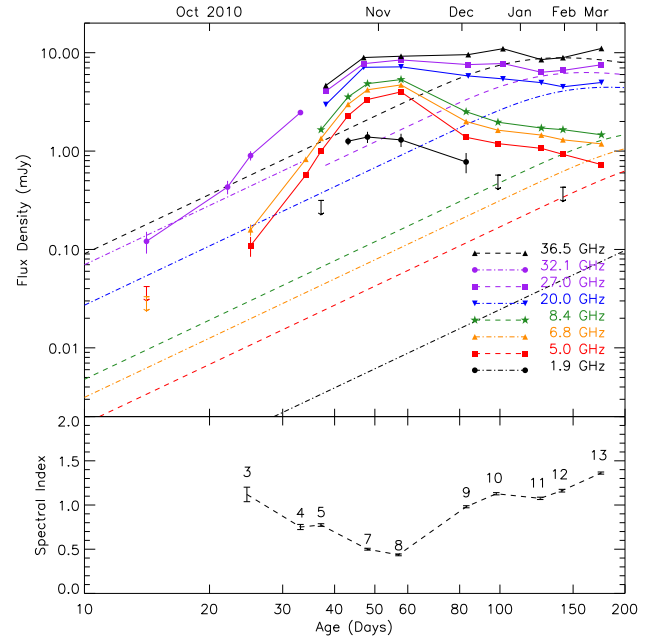


Figure 1. Upper panel: EVLA light curves of V1723 Aql (solid lines; 3σ upper limits are plotted as downward arrows). Dashed and dot-dashed curves show Hubble-flow model light curves for $M_{\text{ej}} = 10^{-4} M_\odot$, $T_{\text{ej}} = 10^4$ K, $v_{\text{ej}} = 1500$ km s⁻¹, and $d = 5$ kpc. Decreasing the distance will raise all model light curves equally in log space, so will not change their spread in frequency or their poor match to the observed fluxes. This discrepancy is due to the fact that the observed spectral index during this time is significantly less than $\alpha = 2$ ($S_\nu \propto \nu^\alpha$), which is the value predicted by the optically-thick rise of the Hubble-flow model. Lower panel: the spectral index α from a single power-law fit to the 4–37 GHz data; each point is labeled by observing epoch.

epoch. The addition of a second power-law is favored at less than 3σ significance, so we use the results from the single power-law fits in our discussion of V1723 Aql. We also plot this spectral index α ($S_\nu \propto \nu^\alpha$) in the lower panel of Figure 1, showing that the rise portion of the light curve is accompanied by a flattening of the spectrum, which then steepens again with the turnover in low-frequency flux. We report the results of our spectral fitting in Table 3.

Table 3
Power-law Spectral Indices of Radio Spectra

Epoch	4–40 GHz		4–9 GHz		19–40 GHz		F-test ^a
	α	χ^2_ν (dof) ^b	α	χ^2_ν (dof)	α	χ^2_ν (dof)	σ
3	1.120 ± 0.082	0.07 (3)
4	0.751 ± 0.029	4.23 (3)
5	0.774 ± 0.015	2.44 (8)	0.978 ± 0.067	0.20 (4)	0.778 ± 0.070	4.52 (2)	0.99
6	0.840 ± 0.031	0.15 (4)
7	0.499 ± 0.011	10.77 (8)	0.710 ± 0.026	0.67 (4)	0.363 ± 0.068	1.53 (2)	2.86
8	0.436 ± 0.010	4.13 (8)	0.551 ± 0.024	0.40 (4)	0.418 ± 0.073	0.95 (2)	2.46
9	0.980 ± 0.012	4.93 (8)	1.133 ± 0.036	3.81 (4)	0.843 ± 0.074	0.56 (2)	1.17
10	1.127 ± 0.013	1.98 (8)	0.956 ± 0.049	0.26 (4)	1.188 ± 0.072	0.62 (2)	2.18
11	1.075 ± 0.013	2.46 (8)	0.912 ± 0.056	0.60 (4)	0.891 ± 0.073	0.41 (2)	2.05
12	1.162 ± 0.015	0.34 (8)	1.116 ± 0.077	0.05 (4)	1.134 ± 0.072	0.98 (2)	0.61
13	1.361 ± 0.012	4.03 (8)	1.281 ± 0.041	6.79 (4)	1.321 ± 0.072	0.21 (2)	0.55

^a The F-test tests the null hypothesis that the reduced χ^2 values are the same for the single- and two-power-law fits, accounting for two fewer degrees of freedom.

^b Reduced χ^2 (degrees of freedom).

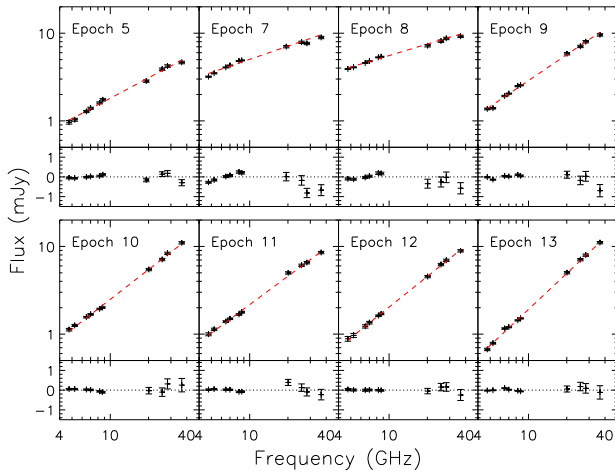


Figure 2. Spectral fits and fit residuals for each epoch where there are flux measurements for 4–37 GHz. Red dashed lines show the single power-law fits for this entire frequency range (residuals are plotted below each spectrum).

3.2. X-ray Modeling

The *Swift* XRT detected 25 (47) events at the position of V1723 Aql on day 41 (61). We estimate 2 ± 4 background counts, resulting in count rates of 7.6 ± 1.6 (7.8 ± 1.2) $\times 10^{-3}$ c s $^{-1}$. We fit the unbinned, non-background subtracted X-ray data with absorbed power-law and thermal bremsstrahlung models in the XSpec spectral fitting package (version 12.6.0) using the Cash statistic (Cash 1979). Although the limited number of counts precludes the determination of well-constrained limits on the fit parameters, the lack of photons with $E < 1$ keV in the first observation, and the appearance of such photons in the second observation, suggests a decreasing absorbing column. The power-law fits find a spectral index of $-2.0^{+2.1}_{-2.2}$ ($-1.4^{+0.9}_{-1.1}$), absorbing column of 11^{+11}_{-8} ($1.3^{+1.9}_{-1.0}$) $\times 10^{22}$ cm $^{-2}$, and flux of $1.3^{+0.4}_{-0.3}$ ($0.9^{+0.3}_{-0.9}$) $\times 10^{-12}$ erg cm $^{-2}$ s $^{-1}$ for the first (second) observation. The thermal bremsstrahlung fits yield similar values for the absorbing column and flux, and place limits on the temperature of the X-ray emitting material in the first (second) observation of $T > 2.1$ (3.4) $\times 10^7$ K (90% confidence).

4. DISCUSSION

A standard model for radio emission from novae envisions a thick, spherical shell of warm ($T \sim 10^4$ K), thermal-bremsstrahlung-emitting ejecta moving away from the white dwarf following the initial explosion (Hjellming et al. 1979). This is often known as the “Hubble-flow” model, since the velocity of the ejecta scales linearly with radial distance from the white dwarf ($v \propto r$). During the rise portion of the nova light curve, the ejecta are optically thick, while the radio photosphere is approximately coincident with the outer shell boundary. This yields a spectrum with $S_\nu \propto \nu^2$ and flux that increases with emitting area ($S_\nu \propto t^2$). As the shell expands, the density falls and the free-free opacity drops, first at high and then at lower frequencies. The source transitions to an optically thin spectrum ($\alpha = -0.1$), with the “width” of the transition, in time or in frequency, proportional to the physical width of the emitting shell.

This model has worked very well for a number of novae, including some that have been imaged with MERLIN and the VLA (e.g., V1500 Cyg, QU Vul, and V723 Cas; Hjellming et al. 1979; Taylor et al. 1988; Heywood et al. 2005). Note that overall shape of light curves determined by the Hubble-flow model is fixed by a small set of parameters: the distance d , ejected mass M_{ej} , ejecta temperature T_{ej} , outer ejecta velocity v_{ej} , and ratio of inner to outer velocity (which is not relevant until late in the light curve evolution). During the rise portion of the light curve, no modification of these parameters will change the fact that the Hubble-flow model predicts an optically thick ($\alpha = 2$) source which increases in flux as t^2 . Neither of these basic characteristics are observed in V1723 Aql. To characterize this discrepancy, we compare our light curves with a set calculated using the Hubble-flow model. We use characteristic values for classical novae of $M_{\text{ej}} = 10^{-4} M_\odot$ and $T_{\text{ej}} = 10^4$ K (e.g., Table 7.2 of Seaquist & Bode 2008), as well as the outer ejecta velocity from optical line widths, $v_{\text{ej}} = 1500$ km s $^{-1}$. So that these light curves do not, at any point, overpredict the observed fluxes, we assume a distance of $d = 5$ kpc. If there is an underlying Hubble-flow component, this assumption allows for its presence in addition to other possible contributions to the flux. Furthermore, changes in the assumed distance, which is otherwise ill-defined for

this nova, will simply scale the flux and will not change the shape of the light curves or the spectral properties.

The observed light curves show a broad “bump” of excess emission relative to these model light curves (Figure 1). The initial rise goes as $t^{3.3}$ —much faster than the expected t^2 from the freely-expanding shell of the Hubble-flow model—while the initial spectrum has $\alpha = 1.1$, substantially shallower than the $\alpha = 2$ expected from its purely optically thick, single-temperature emission. During the time when the bump is present, the spectral index decreases significantly, reaching a minimum of $\alpha \approx 0.4$. The shallow spectral index implies that the source is partially optically thin during the entire bump, over a factor of ~ 100 change in flux density. Most astronomical transients, whether supernovae, quasars, X-ray binaries, or gamma-ray bursts, show rapid increases in flux density only when they are optically thick, and peak when they turn optically thin. Finally, the data during the decline show the spectrum *steepening*, with the flux densities at the higher frequencies remaining almost constant while the flux densities at the lower frequencies drop dramatically. By the time of our last observation, the spectral index had risen to $\alpha = 1.4$. This could be the appearance of the expected Hubble-flow emission. However, the relaxation to a more optically thick spectrum is the opposite of normal behavior from expanding ejecta, where a source becomes more optically thin with time.

This radio behavior — particularly the rapid rise while optically thin — is, to our knowledge, unique among both classical novae and astronomical transients in general. The limited optical and X-ray data show V1723 Aql as a normal, unremarkable classical nova. The radio oddities seen here would have been easily visible in well-sampled light-curves of novae such as V1974 Cyg or FH Ser 1970 (Hjellming 1996), assuming they were of a similar magnitude relative to the observed optically-thick emission.

The radio data do not obviously suggest any emission process beyond thermal bremsstrahlung. Although synchrotron emission can, in principle, produce a wide range of spectral indices, it is commonly seen with a much steeper rise when optically thick ($\alpha = 2.5$) or a falling spectrum when optically thin ($\alpha = -0.5$ to -1). Furthermore, there is no obvious signature of a dense environment which might lead to strong shocks to power the synchrotron emission (as in RS Oph; O’Brien et al. 2006; Rupen et al. 2008; Sokoloski et al. 2008). We do not see evidence for excess emission at low frequencies (~ 1 – 2 GHz), and can place a 3σ upper limit on the linear polarization of $< 39 \mu\text{Jy}$ (or 1%) on day 48, averaging across 1 GHz of bandwidth from 5–6 GHz, and less than 0.36 mJy (or 10%), averaging across a single channel of 2 MHz bandwidth. However, these non-detections are not surprising, considering the high levels of Faraday depolarization expected in the Galactic plane, as well as beam depolarization and depolarization internal to the nova itself.

Assuming the radio emission process is thermal bremsstrahlung, we must make significant revisions to the standard Hubble-flow model to explain our observations. The simplest possibility is that there are two physically distinct emission regions, one giving rise to the bump and the other to the late-time, optically thick emission. The challenge here is that the optically thick mate-

rial cannot obscure the bump emission. Either the source is highly asymmetric, with the bump material physically distinct from the optically thick region (e.g., a bipolar outflow plus an expanding thick ring), or the material producing the bump must lie outside the optically thick region.

If there are physically distinct emitting regions, the optically thick emission might correspond to the early stages (rising flux density part) of a modified Hubble-flow model. The bump is more difficult to explain, since this requires increasing emission from optically *thin* components over time. Thermal bremsstrahlung requires hot ionized gas, and the rapid flux density rise requires rapid physical evolution. One obvious candidate for producing such highly variable hot gas is shocks, either internal to the nova ejecta, or between the ejecta and surrounding circumstellar material (CSM). Both have been proposed for classical novae on other grounds. The presence of internal shocks is motivated by the profiles and evolution of optical line spectra, which indicate that novae eject material in two stages: an initial relatively slow ejection, followed by a faster wind (e.g., Warner 2008). The material in the wind eventually catches up with the initial ejecta, producing shocks with characteristic velocity differentials of up to a few thousand km s^{-1} . Hard X-ray emission (> 1 keV) has also been detected from many classical novae, 5–1000 days after the optical peak (Mukai et al. 2008 and references therein), and this has been modeled as arising from these same internal shocks (O’Brien et al. 1994). Internal shocks have previously been posited to explain early-time radio emission from Nova Vul 1984 No. 2 (Taylor et al. 1987) as well. There is less direct evidence for shocks between the nova ejecta and a surrounding circumstellar medium, but such a CSM has been proposed by Williams & Mason (2010) and would naturally lead to shocks, as are often seen in supernovae.

The *Swift* XRT detected V1723 Aql as a hard ($E > 1$ keV) X-ray source during the time when the bump was seen in the radio light curves, suggesting that strong shocks were present. While the X-ray-emitting gas itself would not produce observable radio emission, hydrodynamical simulations of colliding outflows suggest that the gas behind the shock might contain a range of temperatures as well as regions of high density (O’Brien et al. 1994; see also Lloyd et al. 1996). The required gas densities, temperatures, and total masses are not excessive. At 5 kpc, the observed 8 GHz emission around day 40 could be produced by a shell with thickness $\sim 10^{13}$ cm (outer radius $\sim 5 \times 10^{14}$ cm), density $n_e \sim 10^7 \text{ cm}^{-3}$, temperature $\sim 10^6$ K, and total mass of a few times $10^{-6} M_\odot$. Whether such models can reproduce the observed light curves and spectra remains to be seen. Any successful model must also explain why the bump seen in V1723 Aql is not seen in the radio light curves of other classical novae, although many classical novae show evidence of shocks. These models, and the relation between V1723 Aql and other novae, depend crucially on continued radio monitoring, which will show whether V1723 Aql ultimately follows the canonical Hubble-flow models at late times. Upcoming radio imaging with the EVLA in its most extended, highest resolution “A” configuration will also provide valuable information on the

physical size and geometry of the ejecta.

The National Radio Astronomy Observatory is a facility of the National Science Foundation operated under cooperative agreement by Associated Universities, Inc. We acknowledge with thanks the variable star observations from the AAVSO International database contributed by observers worldwide and used in this research. This research has made use of NASA's Astrophysics Data System Bibliographic Services.

REFERENCES

- Balam, D., Hsiao, E. Y., & Graham, M. 2010, IAU Circ., 9168, 1
- Cash, W. 1979, ApJ, 228, 939
- Gehrels, N. et al. 2004, ApJ, 611, 1005
- Henden, A. A. 2010, private communication
- Heywood, I., O'Brien, T. J., Eyres, S. P. S., Bode, M. F., & Davis, R. J. 2005, MNRAS, 362, 469
- Hjellming, R. M. 1996, in Astronomical Society of the Pacific Conference Series, Vol. 93, Radio Emission from the Stars and the Sun, ed. A. R. Taylor & J. M. Paredes, 174
- Hjellming, R. M., Wade, C. M., Vandenberg, N. R., & Newell, R. T. 1979, AJ, 84, 1619
- Lloyd, H. M., O'Brien, T. J., & Bode, M. F. 1996, in Astronomical Society of the Pacific Conference Series, Vol. 93, Radio Emission from the Stars and the Sun, ed. A. R. Taylor & J. M. Paredes, 200–202
- Mukai, K., Orio, M., & Della Valle, M. 2008, ApJ, 677, 1248
- O'Brien, T. J., Bode, M. F., Porcas, R. W., Muxlow, T. W. B., Eyres, S. P. S., Beswick, R. J., Garrington, S. T., Davis, R. J., & Evans, A. 2006, Nature, 442, 279
- O'Brien, T. J., Lloyd, H. M., & Bode, M. F. 1994, MNRAS, 271, 155
- Payne-Gaposchkin, C. H. 1957, The Galactic Novae.
- Poole, T. S. et al. 2008, MNRAS, 383, 627
- Rupen, M. P., Mioduszewski, A. J., & Sokoloski, J. L. 2008, ApJ, 688, 559
- Seaquist, E. R. & Bode, M. F. Radio emission from novae (Classical Novae, 2nd Edition; edited by M.F. Bode and A. Evans. Cambridge Astrophysics Series, No. 43, Cambridge: Cambridge University Press), 141–164
- Seaquist, E. R., Duric, N., Israel, F. P., Spoelstra, T. A. T., Ulich, B. L., & Gregory, P. C. 1980, AJ, 85, 283
- Seaquist, E. R. & Palimaka, J. 1977, ApJ, 217, 781
- Sokoloski, J. L., Rupen, M. P., & Mioduszewski, A. J. 2008, ApJ, 685, L137
- Taylor, A. R., Hjellming, R. M., Seaquist, E. R., & Gehrz, R. D. 1988, Nature, 335, 235
- Taylor, A. R., Pottasch, S. R., Seaquist, E. R., & Hollis, J. M. 1987, A&A, 183, 38
- Warner, B. Properties of novae: an overview (Classical Novae, 2nd Edition; edited by M.F. Bode and A. Evans. Cambridge Astrophysics Series, No. 43, Cambridge: Cambridge University Press), 16–33
- Williams, R. & Mason, E. 2010, Ap&SS, 327, 207
- Yamanaka, M., Itoh, R., & Komatsu, T. 2010, IAU Circ., 9167, 3